Hydrate phase equilibria of the ternary CH4 + NaCl + Water, CO2 + NaCl + water and CH4 + CO2 + water mixtures in silica Gel pores

ARTICLE *in* THE JOURNAL OF PHYSICAL CHEMISTRY B · DECEMBER 2002

Impact Factor: 3.3 · DOI: 10.1021/jp026776z

2 AUTHORS, INCLUDING:

Yongwon Seo
Ulsan National Institute of Science and Tech…
55 PUBLICATIONS **1,062** CITATIONS

SEE PROFILE

Hydrate Phase Equilibria of the Ternary CH_4 + NaCl + Water, CO_2 + NaCl + Water and CH_4 + CO_2 + Water Mixtures in Silica Gel Pores

Yongwon Seo and Huen Lee*

Department of Chemical and Biomolecular Engineering, Korea Advanced Institute of Science and Technology, 373-1 Guseong-dong Yuseong-gu, Daejeon 305-701, Korea

Received: August 16, 2002; In Final Form: November 25, 2002

Hydrate phase equilibria for the ternary CH_4 + NaCl + water and CO_2 + NaCl + water mixtures in 15.0 nm silica gel pores and for the ternary CH_4 + CO_2 + water mixtures of various CO_2 vapor compositions (20, 40, 60 and 80 mol %) in silica gel pores of nominal diameters 6.0, 15.0, and 30.0 nm were experimentally measured and compared with the calculated results based on van der Waals and Platteeuw model. At a specified temperature, three phase H−L_W−V equilibrium curves of pore hydrates were shifted to a higher pressure region depending on NaCl concentrations and pore sizes. A Pitzer model for electrolytes solutions and a correction term for capillary effect were adopted to estimate the activity of water in the aqueous electrolyte solutions within silica gel pores. The cage dependent ^{13}C NMR chemical shifts of the enclathrated CH_4 molecules in 15.0 nm silica gel pores were confirmed to be identical with those of bulk CH_4 hydrates (sI) and consistent through different NaCl concentrations and CO_2 compositions.

Introduction

Gas hydrates are nonstoichiometric crystalline compounds formed when "guest" molecules of suitable size and shape are incorporated in the well-defined cages in the "host" lattice made up of hydrogen-bonded water molecules. These compounds exist in three distinct structures I (sI), structure II (sII), and structure H (sH), which contain differently sized and shaped cages. The sI and sII hydrates consist of two types of cages, whereas the sH hydrate consists of three types of cages.[1]

Gas hydrates are of particular interest in the petroleum industry as well as in energy and environmental field. Large masses of natural gas hydrates exist in the permafrost region or beneath deep oceans, where they were commonly found in sediment pores. Because each volume of hydrate can contain as much as 170 volumes of gas at standard temperature and pressure conditions, naturally occurring gas hydrates in the earth containing mostly CH_4 are regarded as future energy resources.[1] The recent investigations have suggested the possibility of sequestering industrially produced CO_2 as crystalline gas hydrates in the deep ocean to prevent further release into the atmosphere as a greenhouse gas.[2] It has been also investigated that the injection of CO_2 into CH_4 hydrate reserves could result in simultaneous process merits of both CO_2 sequestration and CH_4 exploitation.[3] Because these natural phenomena of hydrate formation/substitution occur in deep ocean sediments, it becomes essential to consider the complicated effects of both porous media and electrolytes on the formation of simple and mixed hydrates. However, any research work on simple and mixed hydrates containing electrolytes in porous media has not yet appeared in the literature, even though numerous investigations covering separately either porous medium or electrolyte effect have been found from various sources.[1,4−9] The cage substitution mechanism between CH_4 and CO_2 molecules might be thought to be easily tractable, but for its complete understanding, both equilibrium and nonequilibrium approaches are required in the bulk and porous medium surroundings. Moreover, the highly complex phase behavior of mixed hydrate systems containing multiguest components must be explored as a priori to examine the feasibility of natural gas exploitation in connection with CO_2 sequestration.

In this connection, the present work was newly attempted to provide fundamental key information of electrolyte effects on hydrate phase equilibrium behavior, particularly, in porous media. First, the hydrate phase equilibria of two ternary CH_4 + NaCl + water and CO_2 + NaCl + water mixtures were measured in 15.0 nm silica gel pores at three different NaCl concentrations of 3, 5, and 10 wt % to secure fundamental electrolyte role on simple hydrate formation occurring in pores. Second, the hydrate phase equilibria of the CH_4 + CO_2 + water mixture in 15.0 nm silica gel pores were also carefully determined at CO_2 compositions of 20, 40, 60, and 80 mol % in order to meet changeable surroundings of sea floor and sediments. Third, three different silica gels of nominal diameters 6.0, 15.0, and 30.0 nm were used to check pore-size effects on hydrate equilibrium. All of these measured data were compared with calculated values based on the van der Waals and Platteeuw model incorporated with two additional terms considering electrolytes and pores. Furthermore, the ^{13}C NMR spectra were examined to identify and confirm the hydrate structure of the CH_4 + NaCl + water and CH_4 + CO_2 + water mixtures formed in silica gel pores.

Experimental Section

Materials. CO_2 gas of 99.9 mol % purity was supplied by World Gas (Korea), and CH_4 gas with a minimum purity of 99.95 mol % was supplied by Linde Gas UK Ltd (UK). The CH_4 + CO_2 gas mixtures (20, 40, 60, and 80 mol % CO_2) were supplied by World Gas (Korea), and their compositions were checked again. The water with ultrahigh purity was supplied by Merck (Germany). Silica gels of nominal pore diameter 6.0 nm (6.0 nm SG) and 15.0 nm (15.0 nm SG) were purchased

* To whom correspondence should be addressed. Phone: 82-42-869-3917. Fax: 82-42-869-3910. E-mail: hlee@mail.kaist.ac.kr.

10.1021/jp026776z CCC: $25.00
Published on Web 12/21/2002

from Aldrich (USA), and 30.0 nm silica gel (30.0 nm SG) was purchased from Silicycle (Canada). All materials were used without further treatment. The properties of silica gels having three different pore diameters were measured by ASAP 2000 (Micromeritics, USA). The details of the physical properties and pore-size distributions were given in the previous paper.[9]

Apparatus and Procedure. The used silica gels were first dried at 373 K for 24 h before water sorption. Then, the pore saturated silica gels were prepared by placing these dried silica gels in a desiccator containing degassed and distilled water, evacuating the desiccator, and allowing more than 5 days in order to establish the solid−vapor equilibrium. The total amount of sorbed water in the silica gel pores was confirmed by measuring the mass of silica gels before and after saturation and found to be almost identical with the pore volume of each silica gel. For preparing silica gels containing NaCl solution, we followed the same method suggested by Uchida et al.[5] The amount of electrolyte solution equivalent to total pore volume of dried silica gels was added to the sample contained in the bottle. After being mixed, the mixture was sealed off with a cap to prevent water evaporation. To facilitate water filling into the pores, the bottle with the mixture was vibrated and warmed for 24 h with an ultrasonic wave. The validity of this method was verified by comparing the experimental results obtained from two different methods.

A schematic diagram and detailed description of the experimental apparatus for hydrate phase equilibria was given in the previous papers.[10,11] The apparatus was specially constructed to measure accurately the hydrate dissociation pressures and temperatures. The equilibrium cell was made of 316 stainless steel and had an internal volume of about 50 cm^3. The experiment for hydrate-phase equilibrium measurements began by charging the equilibrium cell with about 25 cm^3 of silica gels containing pore water. After the equilibrium cell was pressurized to a desired pressure with gas, the whole main system was slowly cooled to about 10 K below the expected hydrate-formation temperature. When pressure depression due to hydrate formation reached a steady-state condition, the cell temperature was increased at a rate of about 0.1 K/h. The nucleation and dissociation steps were repeated at least two times in order to reduce hysteresis phenomenon. The equilibrium pressure and temperature of three phases (hydrate (H)−water-rich liquid (L_W)−vapor (V)) were determined by tracing the $P-T$ profiles from hydrate formation to dissociation. Unlike the bulk hydrate, in case of hydrates in silica gel pores, a gradual change of slope around the final hydrate dissociation point was observed because of the pore-size distribution. As a consequence, it becomes, of course, very difficult to determine the unique equilibrium dissociation point in the $P-T$ profile measured for the silica gel pores. To overcome these inherent difficulties, the dissociation equilibrium point in silica gel pores was chosen in the present study as the cross point between the maximum inclination line and complete dissociation line. As indicated by Uchida et al.,[5] this unique point corresponds to the dissociation one in the pores of the mean diameter of used silica gels.

To identify the hydrate structure of the CH_4 + NaCl + water and CH_4 + CO_2 + water mixtures in silica gel pores, a Bruker 400 MHz solid-state NMR spectrometer was used in this study. The NMR spectra were recorded at 200 K by placing the hydrate samples within a 4 mm o.d. Zr-rotor that was loaded into the variable temperature (VT) probe. All ^{13}C NMR spectra were recorded at a Larmor frequency of 100.6 MHz with magic angle spinning (MAS) at about 2−4 kHz. The pulse length of 2 μs and pulse repetition delay of 20 s under proton decoupling were employed when the radio frequency field strengths of 50 kHz corresponding to 5 μs 90° pulses were used. The downfield carbon resonance peak of adamantane, assigned a chemical shift of 38.3 ppm at 300 K, was used as an external chemical shift reference.

Thermodynamic Model. The equilibrium criteria of the hydrate-forming mixture are based on the equality of fugacities of the specified component i in all phases which coexist simultaneously

$$\hat{f}_i^{\,H} = \hat{f}_i^{\,L} = \hat{f}_i^{\,V} (= f_w^I) \tag{1}$$

where H stands for the hydrate phase, L for the water-rich liquid phase, V for the vapor phase and I for the ice phase. It can be reasonably assumed that electrolytes are completely excluded from hydrate lattice and remain only in the liquid phase.

The chemical potential difference between the empty hydrate and filled hydrate phases, $\Delta\mu_w^{MT-H}$ ($=\mu_w^{MT} - \mu_w^H$), is generally derived from statistical mechanics in the van der Waals and Platteeuw model[12]

$$\Delta\mu_w^{MT-H} = \mu_w^{MT} - \mu_w^H = -RT\sum_m \nu_m \ln(1 - \sum_j \theta_{mj}) \tag{2}$$

where ν_m is the number of cavities of type m per water molecule in the hydrate phase and θ_{mj} is the fraction of cavities of type m occupied by the molecules of component j.

Holder et al.[13] suggested the method to simplify the chemical potential difference between empty hydrate and reference state as follows:

$$\frac{\Delta\mu_w^{MT-I}}{RT} = \frac{\Delta\mu_w^0}{RT} - \int_{T_0}^{T}\frac{\Delta h_w^{MT-I}}{RT^2}\,dT + \int_0^P \frac{\Delta v_w^{MT-I}}{RT}\,dP \tag{3}$$

$$\frac{\Delta\mu_w^{MT-L}}{RT} = \frac{\Delta\mu_w^0}{RT} - \int_{T_0}^{T}\frac{\Delta h_w^{MT-I} + \Delta h_w^{fus}}{RT^2}\,dT + \int_0^P \frac{\Delta v_w^{MT-I} + \Delta v_w^{fus}}{RT}\,dP - \ln a_w \tag{4}$$

where T_0 is 273.15 K, the normal melting point of water, $\Delta\mu_w^0$ is the chemical potential difference between empty hydrate and water at T_0 and zero absolute pressure, Δh_w^{MT-I} and Δv_w^{MT-I} are the molar differences in enthalpy and volume between empty hydrate and ice, respectively, and Δh_w^{fus} and Δv_w^{fus} are the molar differences in enthalpy and volume between ice and liquid water, respectively. a_w denotes the activity of water calculated from an equation of state and is equivalent to the product of activity coefficient of water and salt-free mole fraction of water, x_w.

The fugacity of water in the filled hydrate lattice, $\hat{f}_w^{\,H}$, is calculated by either of the following two expressions depending on the equilibrium temperature. If the equilibrium temperature is below the ice point

$$\hat{f}_w^{\,H} = f_w^{\,I} \exp\left(\frac{\Delta\mu_w^{MT-I}}{RT} - \frac{\Delta\mu_w^{MT-H}}{RT}\right) \tag{5}$$

and above the ice point

$$\hat{f}_w^{\,H} = f_w^{\,L} \exp\left(\frac{\Delta\mu_w^{MT-L}}{RT} - \frac{\Delta\mu_w^{MT-H}}{RT}\right) \tag{6}$$

where $\Delta\mu_w^{MT-I} = \mu_w^{MT} - \mu_w^{I}$ and $\Delta\mu_w^{MT-L} = \mu_w^{MT} - \mu_w^{L}$, respectively.

The fugacity coefficient of water, φ_w, in the aqueous electrolyte liquid phase is given by the model of Aasberg-Petersen et al.[14]

$$\ln \varphi_w = \ln \varphi_w^{EOS} + \ln \gamma_w^{EL} \quad (7)$$

The first term for normal contribution can be calculated from SRK-EOS, and the second term for electrolyte contribution can be calculated from the Pitzer model[15]

$$\gamma_w^{EL} = a_w^{EL}/x_w \quad (8)$$

$$\ln a_w^{EL} = -\frac{M_w \nu m}{1000}\phi \quad (9)$$

where a_w^{EL} stands for activity of water in electrolytes solution, M_w stands for the molecular weight of water, m stands for the molality of the electrolyte, ν stands for the number of ions the electrolytes dissociates into, and ϕ stands for the osmotic coefficient. The osmotic coefficient for single electrolyte solution is as follows:

$$\phi - 1 = |z_+ z_-| f^\phi + m\left(\frac{2\nu_+\nu_-}{\nu}\right)B_\pm{}^\phi + m^2\left[\frac{2(\nu_+\nu_-)^{3/2}}{\nu}\right]C_\pm{}^\phi \quad (10)$$

$$f^\phi = -A_\phi \frac{\sqrt{I}}{1 + 1.2\sqrt{I}} \quad (11)$$

where A_ϕ is the Debye−Hückel constant for the osmotic coefficient, I is the ionic strength, ν_i is the number of ion i in the electrolyte, and z_i is the charge on ion i. The binary and ternary ion interaction parameters, $B_\pm{}^\phi$ and $C_\pm{}^\phi$, respectively, are obtained from the complicated empirical best-fit curves.[16]

The decrease of water activity in silica gel pores due to capillary effect occurring by the presence of geometrical constraints can be expressed as[17−20]

$$\ln a_w = \ln a_w^{EL} - \frac{V_L 2\cos\theta\,\sigma_{HW}}{rRT} \quad (12)$$

where V_L is the molar volume of pure water, θ *is* the wetting angle between hydrate and liquid water phases, σ_{HW} is the interfacial tension between hydrate and liquid water phases, and r is the pore radius. More details of the model description were given in our previous papers.[9,21−23]

Results and Discussion

Three-phase H−L_W−V equilibria for the ternary CH_4 + NaCl + water and CO_2 + NaCl + water mixtures in 15.0 nm silica gel pores were measured at the NaCl concentration ranges of 3−10 wt % and presented along with model calculations in Figures 1 and 2 and Table 1. As expected, the presence of either geometrical constraints or electrolytes caused the H−L_W−V curves to be shifted more to the inhibition region represented by the lower temperature and higher pressure condition when compared with the ones in the either bulk or pure state. However, in the present work, the combined effects of porous media and electrolytes that closely simulate real marine sediments were examined through checking the shift of the experimentally measured H−L_W−V curve. Although the experimental determinations of the binary CO_2 + NaCl + water mixtures in silica gel pores were restricted to the H−L_W−V phase boundary, the model calculation could be extended to two different three-phase boundaries of hydrate (H)−ice (I)−vapor (V) and hydrate (H)−water-rich liquid (L_W)−carbon dioxide-rich liquid (L_{CO2}). The upper quadruple point (Q_2) where two H−L_W−V and H−L_W−L_{CO2} phase boundaries intersect and thus four phases (H, L_W, L_{CO2}, and V) coexist was found at the location very close to the corresponding saturation vapor pressure of CO_2.

Of course, the melting point of ice is affected by the presence of geometrical constraints and electrolytes. The lower quadruple point (Q_1) where four phases (H, I, L_W, and V) coexist appears normally adjacent to the corresponding melting point of ice. Therefore, Q_1 is known to be a function of pore radius and electrolyte concentration. In the present study, the values of Q_1

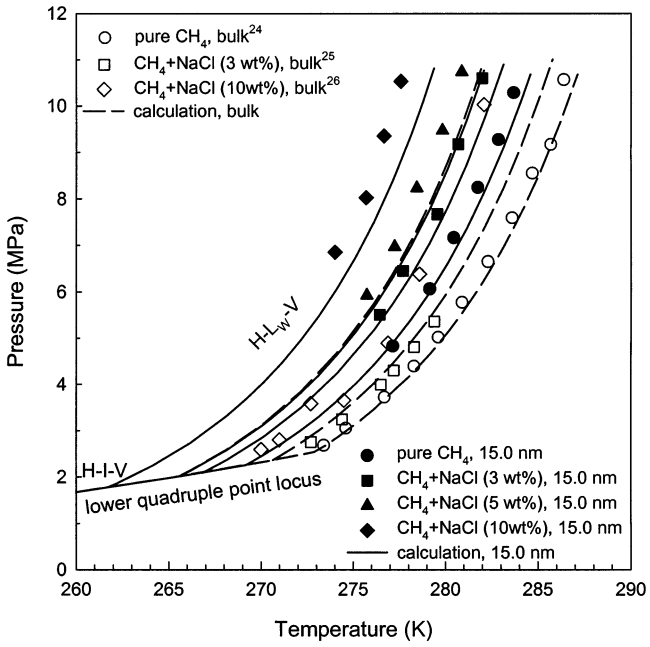

Figure 1. Hydrate phase equilibria of the ternary CH_4 + NaCl + water mixtures in 15.0 nm silica gel pores.

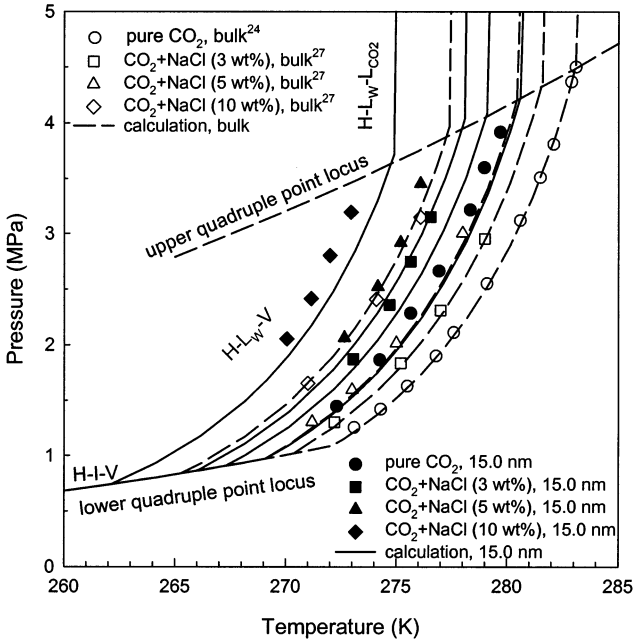

Figure 2. Hydrate phase equilibria of the ternary CO_2 + NaCl + water mixtures in 15.0 nm silica gel pores.

TABLE 1: Hydrate Phase Equilibrium Data for CH_4 + NaCl + Water and CO_2 + NaCl + Water Mixtures in 15.0 nm Silica Gel Pores

NaCl 3 wt %		NaCl 5 wt %		NaCl 10 wt %	
T (K)	*P* (MPa)	*T* (K)	*P* (MPa)	*T* (K)	*P* (MPa)
CH_4 + NaCl + Water Mixtures					
276.45	5.505	275.75	5.93	274.02	6.85
277.7	6.45	277.25	6.97	275.7	8.025
279.55	7.67	278.45	8.23	276.68	9.353
280.7	9.175	279.85	9.472	277.6	10.53
282.0	10.60	280.9	10.74		
CO_2 + NaCl + Water Mixtures					
273.05	1.873	272.65	2.063	270.05	2.053
274.69	2.359	274.17	2.523	271.15	2.415
275.65	2.748	275.2	2.92	272.0	2.802
276.55	3.153	276.1	3.455	272.95	3.195
277.4	3.617				

TABLE 2: Calculated Lower (Q_1) and Upper (Q_2) Quadruple Points

		Q_1		Q_2	
system	NaCl (wt %)	*T* (K)	*P* (MPa)	*T* (K)	*P* (MPa)
CH_4 + NaCl + water, bulk	0	272.9	2.536		
	3	270.65	2.363		
	10	265.55	2.014		
CH_4 + NaCl + water, 15.0 nm	0	269.2	2.258		
	3	266.85	2.092		
	5	265.6	2.020		
	10	261.7	1.775		
CO_2 + NaCl + water, bulk	0	272.1	1.089	283.1	4.522
	3	270.4	1.025	281.6	4.366
	5	269.05	0.97	280.45	4.205
	10	265.25	0.837	277.4	3.964
CO_2 + NaCl + water, 15.0 nm	0	269.1	0.972	280.6	4.230
	3	267.3	0.909	279.1	4.086
	5	266.0	0.865	278.1	4.041
	10	262.15	0.742	274.9	3.717

were not experimentally measured but calculated by the proposed model. The lower quadruple temperatures (T_{Q1}) of CH_4 (or CO_2) + NaCl + water mixtures in 15.0 nm silica gel pores decreased from that of CH_4 (or CO_2) + water mixtures in 15.0 nm pores as the NaCl concentration increased. In the present study, T_{Q1} was determined as the intersection point of two calculated H−L_W−V and H−I−V phase boundaries. The calculated quadruple points of the ternary CH_4 + NaCl + water and CO_2 + NaCl + water mixtures in bulk state and silica gel pores were listed in Table 2.

Three-phase H−L_W−V equilibria for the ternary CH_4 + CO_2 + water mixtures of various CO_2 vapor compositions (20, 40, 60, and 80 mol %) in 15.0 nm silica gel pores were also measured and presented along with model calculations in Figure 3 and Table 3. As generally expected, the H−L_W−V lines of the ternary CH_4 + CO_2 + water mixtures existing between those of the binary CH_4 + water and CO_2 + water mixtures showed the pore inhibition. In particular, three-phase H−L_W−V equilibria for the ternary CH_4 + CO_2 + water mixtures of 40 mol % CO_2 in silica gel pores of nominal diameters 6.0, 15.0, and 30.0 nm were represented along with model calculations in Figure 4 and listed in Table 4. The decrease of pore diameter made the H−L_W−V equilibrium line more shifted toward higher pressure region at a specified temperature.

In porous media, water activity is depressed by partial ordering and bonding of water molecules with hydrophilic pore surfaces.[18] The decrease of water activity leads the hydrate formation condition either to much higher pressure at a specified temperature or to much lower temperature at a specified pressure. This phenomenon is also observed in the mixtures containing inhibitors such as electrolytes and alcohols which cause a depression in the freezing point of water thereby

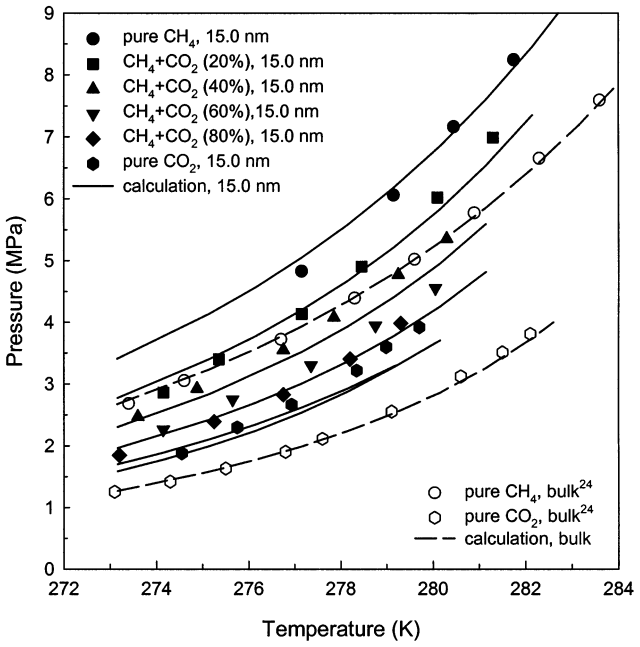

Figure 3. Hydrate phase equilibria of the ternary CH_4 + CO_2 + water mixtures of various CO_2 compositions (20, 40, 60, and 80 mol %) in 15.0 nm silica gel pores.

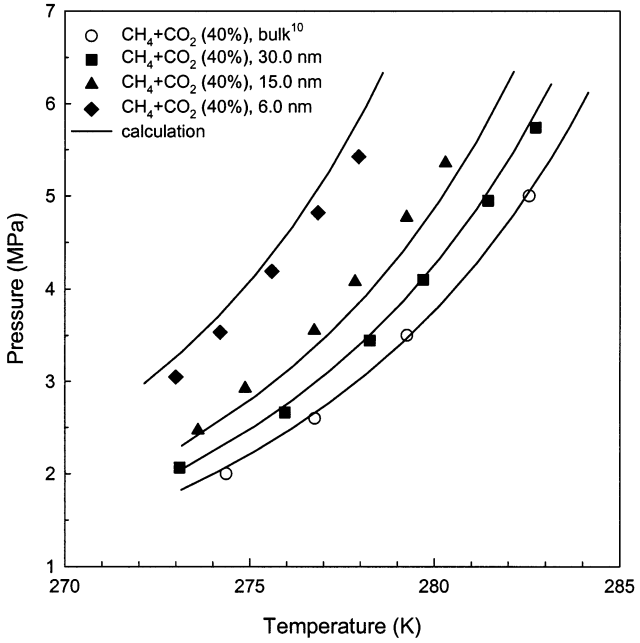

Figure 4. Hydrate phase equilibria of the ternary CH_4 + CO_2 + water mixtures of 40 mol % CO_2 in silica gel pores (6.0, 15.0, and 30.0 nm).

TABLE 3: Hydrate Phase Equilibrium Data for CH_4 + CO_2 + Water Mixtures in 15.0 nm Silica Gel Pores

20 mol % CO_2		40 mol % CO_2		60 mol % CO_2		80 mol % CO_2	
T (K)	*P* (MPa)	*T* (K)	*P* (MPa)	*T* (K)	*P* (MPa)	*T* (K)	*P* (MPa)
274.15	2.86	273.6	2.47	274.15	2.26	273.2	1.843
275.35	3.398	274.88	2.926	275.65	2.747	275.25	2.387
277.15	4.135	276.75	3.552	277.35	3.298	276.75	2.825
278.45	4.905	277.85	4.08	278.75	3.942	278.2	3.401
280.1	6.02	279.25	4.769	280.05	4.55	279.3	3.98
281.3	6.99	280.3	5.355				

TABLE 4: Hydrate Phase Equilibrium Data for $CH_4 + CO_2$ + Water Mixtures of 40 Mol % CO_2 in Silica Gel Pores

6.0 nm SG		15.0 nm SG		30.0 nm SG	
T (K)	P (MPa)	T (K)	P (MPa)	T (K)	P (MPa)
273.0	3.047	273.6	2.47	273.1	2.067
274.2	3.533	274.88	2.926	275.95	2.665
275.6	4.191	276.75	3.552	278.25	3.445
276.85	4.82	277.85	4.08	279.7	4.10
277.95	5.425	279.25	4.769	281.45	4.948
		280.3	5.355	282.73	5.74

reducing its activity. Therefore, the pore effect of geometrical constraints on water activity can be considered to be equivalent to a change in activity as caused by the inhibitors.[4]

A significant proportion of water in the wall of confined spaces has been often found to exist as bound water without undergoing complete freezing transition.[28] This bound water will not also participate in hydrate formation under the same pressure−temperature conditions as the pore water. In the present experiments, the pores of silica gels were first completely saturated with water, and after reaching the H−L_W−V equilibrium, they are filled only with hydrate and liquid water. It is assumed that the wetting angle (θ) is 0°. Even though the operative interface of hydrate and liquid water phases plays a key role in understanding the pore effect on hydrate formation, no reliable data of the interfacial tension between hydrate and liquid water phases (σ_{HW}) have been reported in the literature. According to previous works, the interfacial tension between hydrate and liquid water phases was assumed to be equivalent to that between ice and liquid water phases ($\sigma_{HW} = \sigma_{IW} = 0.027$ J/m^2),[8,18−20] which resulted in large discrepancies between the experimental and calculated values. Recently, Uchida et al.[6] presented the values of σ_{HW} from fitting their experimental values by the Gibbs−Thomson equation: 0.017 J/m^2 for CH_4 hydrate and 0.014 J/m^2 for CO_2 hydrate. By using the values suggested by Uchida et al.,[6] it was found that the predicted H−L_W−V values of pure CH_4 and CO_2 hydrates in silica gel pores were in much better agreement with our experimental ones.[9] To establish the proper interpretation of mixed hydrates in porous media, the values of interfacial tension between hydrate and liquid water phase (σ_{HW}) for $CH_4 + CO_2$ mixed hydrates must be obtained from either theoretical or possibly experimental methods but, unfortunately, up to now, have not yet been reported. Accordingly, in this work, the mole additivity of CH_4 and CO_2 compositions was adopted to determine the following values of interfacial tension: 0.0164 J/m^2 for 20 mol %, 0.0158 J/m^2 for 40 mol %, 0.0152 J/m^2 for 60 mol %, and 0.0146 J/m^2 for 80 mol % (CO_2 basis). By applying this method, the calculated values agreed well with the experimental ones, and the least %AAD was observed for the overall $CH_4 + CO_2$ + water mixtures.

For the prediction of the H−I−V equilibrium lines, the interfacial tension between ice and hydrate phases (σ_{IH}) was assumed to be zero for all of the mixtures. At the present time, the exact nature of σ_{IH} still remains unsolved, and to clarify this point, a more sensitive and accurate experiment will be required for various pore sizes. However, some previous researchers also assumed the value of σ_{IH} to be zero for calculation of the H−I−V equilibria and indirectly confirmed the validity of this assumption by finding that the H−I−V equilibria in porous media was the same as those in the bulk phase.[6,8,19,29] Though the present pore hydrate model was proven to be quite reliable in both qualitative and quantitative manners, the percent average absolute deviations (%AADs) between experimental and calculated H−L_W−V values were listed in Table 5 for reference. The calculated results agreed well with the experimental data, but a little larger deviations were observed at higher concentration of NaCl, higher composition of CO_2, and smaller pore size. These deviations might be attributed to a much larger proportion of bound water existing in the smaller pores, which may cause more experimental errors in the smaller pore sizes, intrinsic limitation of the Pitzer model at higher NaCl concentration, and a large solubility of carbon dioxide in aqueous solutions.[21,28,30] More importantly, the more accurate values of σ_{HW} must be anyhow provided for better improvement.

TABLE 5: Percent AAD between the Experimental and Calculated Values of H−L_W−V Equilibria

system	NaCl (wt %)	%AAD
CH_4 + NaCl + water, 15.0 nm	0	3.92
	3	6.44
	5	10.58
	10	13.6
CO_2 + NaCl + water, 15.0 nm	0	6.32
	3	9.41
	5	10.37
	10	11.24
system	CO_2 (mol %)	%AAD
$CH_4 + CO_2$ + water, 15.0 nm	20	3.55
	40	5.46
	60	6.79
	80	11.86
system	pore diameter (nm)	%AAD
$CH_4 + CO_2$ + water, CO_2 40 mol %	6.0	5.84
	15.0	5.46
	30.0	1.73

The objective of the NMR measurement in this study is to identify and confirm the structure of the CH_4 + NaCl + water and $CH_4 + CO_2$ + water mixtures in porous media. A cage dependent ^{13}C NMR chemical shift of the enclathrated CH_4 molecules can be used to determine structure types of the formed hydrates.[31] From the preliminary experiments, the structure and hydration number of CH_4 hydrates in silica gel pores (6.0, 15.0 and 30.0 nm) were found to be identical with those of bulk CH_4 hydrate.[9] For the CH_4 + NaCl + water and $CH_4 + CO_2$ + water mixtures in 15.0 nm silica gel pores, the positions of two peaks from CH_4 molecules trapped in large and small cages of hydrate lattice were also confirmed to be identical with those of bulk CH_4 hydrates (sI) and consistent through different NaCl concentrations and CO_2 compositions. The cage occupancy behavior occurring in the mixed hydrates is expected to be highly complex. Even though this part is very fundamental on hydrate area, the detailed and organized research has not yet been done so far. Therefore, the macro and micro approaches for investigating hydration number, cage occupancy, and ratio of peak areas in the mixed hydrates need to be attempted in the future. The present NMR works in the porous and electrolyte state is the first one and might be extended to various types of mixed hydrates in order to explore their physicochemical aspects.

Conclusion

Three-phase H−L_W−V equilibria for the ternary CH_4 + NaCl + water and CO_2 + NaCl + water mixtures in 15.0 nm silica gel pores and for the ternary $CH_4 + CO_2$ + water mixtures of various CO_2 compositions in silica gel pores with nominal diameters of 6.0, 15.0, and 30.0 nm were newly measured and compared with model calculations. The presence of geometrical constraints and electrolytes made H−L_W−V equilibrium lines

shifted to higher pressure region at a specified temperature. A Pitzer model for electrolytes solutions and a correction term for capillary effect were adopted to estimate the activity of water in the aqueous electrolyte solutions within silica gel pores. The hydrate structures of the CH_4 + NaCl + water and CH_4 + CO_2 + water mixtures in 15.0 nm silica gel pores were confirmed to be identical with that of the CH_4 + water mixture in bulk state through ^{13}C NMR spectroscopy. The overall phase behavior considering the combined effects of pore and electrolyte could provide key information for exploiting natural gas hydrates from marine sediments, substituting carbon dioxide molecules into gas hydrate reservoirs, and sequestering carbon dioxide into sea floor as solid hydrates.

Acknowledgment. This research was performed for the Greenhouse Gas Research Center, one of the Critical Technology-21 Programs, funded by the Ministry of Science and Technology of Korea and also partially supported by the Brain Korea 21 Project.

References and Notes

(1) Sloan, E. D. *Clathrate Hydrates of Natural Gas*, 2nd edition, revised and expanded; Dekker: New York, 1998.
(2) Teng, H.; Yamasaki, A.; Chun, M. K.; Lee, H. *Energy* **1997**, *22*, 1111.
(3) Ohgaki, K.; Takano, K.; Sangawa, H.; Matsubara, T.; Nakano, S. *J. Chem. Eng. Jpn.* **1996**, *29*, 478.
(4) Handa, Y. P.; Stupin, D. *J. Phys. Chem.* **1992**, *96*, 8599.
(5) Uchida, T.; Ebinuma, T.; Ishizaki, T. *J. Phys. Chem. B* **1999**, *103*, 3659.
(6) Uchida, T.; Ebinuma, T.; Takeya, S.; Nagao, J.; Narita, H. *J. Phys. Chem. B* **2002**, *106*, 820.
(7) Seshadri, K.; Wilder, J. W.; Smith, D. H. *J. Phys. Chem. B* **2001**, *105*, 2627.
(8) Smith, D. H.; Wilder, J. W.; Seshadri, K. *AIChE J*. **2002**, *48*, 393.
(9) Seo, Y.; Lee, H.; Uchida, T. *Langmuir* **2002**, *18*, 9164.
(10) Seo, Y.-T.; Lee, H. *J. Phys. Chem. B* **2001**, *105*, 10084.
(11) Seo, Y.; Lee, H. *Environ. Sci. Technol.* **2001**, *35*, 3386.
(12) van der Waals, J. H.; Platteeuw, J. C. *Adv. Chem. Phys*. **1959**, *2*, 1.
(13) Holder, G. D.; Corbin, G.; Papadopoulos, K. D. *Ind. Eng. Chem. Fundam*. **1980**, *19*, 282.
(14) Aasberg-Petersen, K.; Stenby, E.; Fredenslund, A. *Ind. Eng. Chem. Res.* **1991**, *30*, 2180.
(15) Pitzer, K. S. *J. Phys. Chem.* **1973**, *77*, 268.
(16) Pitzer, K. S.; Mayorga, G. *J. Phys. Chem*. **1973**, *77*, 2300.
(17) Clarke, M. A.; Pooladi-Darvish, M.; Bishnoi, P. R. *Ind. Eng. Chem. Res.* **1999**, *38*, 2485.
(18) Henry, P.; Thomas, M.; Clennell, M. B. *J. Geophys. Res*. **1999**, *104*, 23005.
(19) Wilder, J. W.; Seshadri, K.; Smith, D. H. *Langmuir* **2001**, *17*, 6729.
(20) Klauda, J. B.; Sandler, S. I. *Ind. Eng. Chem. Res.* **2001**, *40*, 4197.
(21) Kang, S. P.; Chun, M. K.; Lee, H. *Fluid Phase Equilibr*. **1998**, *147*, 229.
(22) Chun, M. K.; Lee, H. *J. Chem. Eng. Data* **2000**, *45*, 1150.
(23) Yoon, J. H.; Chun, M. K.; Lee, H. *AIChE J*. **2002**, *48*, 1317.
(24) Adisasmito, S.; Frank, R. J.; Sloan, E. D. *J. Chem. Eng. Data* **1991**, *36*, 68.
(25) Dholabhai, P. D.; Englezos, P.; Kalogerakis, N.; Bishnoi, P. R. *Can. J. Chem. Eng*. **1991**, *69*, 800.
(26) Kobayashi, R.; Withrow, H. J.; Williams, G. B.; Katz, D. L. *Proc. NGAA* **1951**, *1951*, 27.
(27) Dholabhai, P. D.; Kalogerakis, N.; Bishnoi, P. R. *J. Chem. Eng. Data* **1993**, *38*, 650.
(28) Handa, Y. P.; Zakrzewski, M.; Fairbridge, C. *J. Phys. Chem*. **1992**, *96*, 8594.
(29) Zhang, W.; Wilder, J. W.; Smith, D. H. *Proc. 4th Int Conf. Gas Hydrates* **2002**, *1*, 321.
(30) Prausnitz, J. M.; Lichtenthaler, R. N.; Azevedo, E. G. *Molecular Thermodynamics of Fluid-Phase Equilibria*, 3rd edition; Prentice Hall: New York, 1999.
(31) Ripmeester, J. A.; Ratcliffe, C. I. *J. Phys. Chem*. **1988**, *92*, 337.